



Supplement of

Characteristics and degradation of organic aerosols from cooking sources based on hourly observations of organic molecular markers in urban environments

Rui Li et al.

Correspondence to: Li Li (lily@shu.edu.cn)

The copyright of individual parts of the supplement might differ from the article licence.

1

2

3

4

5

6

7

8

9

10

11

12 CONTENTS

13 **Section S1. Source analysis using PMF.**

14 **Figure S1. Time series of PM_{2.5} and its components and organic molecular tracers.**

15 **Figure S2. The variation of the total spatial variance.**

16 **Figure S3. Day-to-day fitting of oleic acid normalized by palmitic acid.**

17 **Figure S4. Day-to-day fitting of linoleic acid normalized by palmitic acid.**

18 **Figure S5. Individual source profiles of the 11 factors resolved in the constrained PMF run (a) and time series of individual
19 factor contributions (b).**

20 **Figure S6. Diurnal variation in individual source factors resolved by PMF.**

21 **Table S1. Contribution of TFAs to total OC from different sources.**

22 **Table S2. Naming of molecular markers included in the PMF analysis.**

23 **Table S3. Summary of error estimation diagnostics from BS, DISP and BS-DISP for PMF.**

24

25

26 **Section S1. Source analysis using PMF.**

27 Table S2 lists the input data ($\text{PM}_{2.5}$ and its components) in the PMF modeling. The preferential input species for
28 PMF are those with high abundance and source specific (Norris et al., 2014). Generally, organic markers with lower
29 volatility and lower reactivity were selected. Figure S5 shows the individual source profiles of the 10 factors resolved in
30 the PMF (a) and time series of individual factor contributions (b). Figure S6 shows the diurnal variation in individual
31 source factors resolved by PMF. Table S3 shows the summary of error estimation diagnostics from bootstrap (BS),
32 displacement (DISP), and bootstrap combined with displacement (BS–DISP) for the PMF base run. Generally, BS and
33 DISP results indicated robust PMF solutions. However, BS–DISP results showed higher uncertainties which may be due
34 to the limited sample size in the study. It should be noted that secondary nitrate and secondary sulfate showed the lowest
35 BS mappings and a high chance of mixing with the vehicle exhaust, industry emission and coal combustion factors. Here,
36 we only briefly present the identification of each source factor.

37 A total of 10 factors are identified. Among them, seven are primary sources, they are industrial emission, biomass
38 burning, vehicle exhaust, coal combustion, dust, cooking and fire working. Three secondary sources, namely, secondary
39 nitrate, secondary sulfate and SOA factor (Li et al., 2020; Wang et al., 2017).

40 Secondary nitrate factor is identified by high contributions of nitrate and ammonium. The secondary sulfate factor is
41 characterized by high loadings of sulfate and ammonium. The SOA factor is characterized by high loadings of an
42 anthropogenic SOA tracer (phthalic acid), isoprene SOA tracer (2-methylglyceric acid) and α -pinene SOA tracers (3-
43 hydroxyglutaric acid, pinic acid and cis-pinonic acid) (Wang et al., 2017). The profile of industrial emission contains
44 high loadings of Cr, Zn, Fe and Mn (Men et al., 2019; Pant and Harrison, 2013). Industry activities related to steel
45 production, plating, and metallurgy often emit a large amount of these metallic elements. Biomass burning is identified
46 by high loadings of levoglucosan and mannosan (Feng et al., 2013; Wang et al., 2019). The seventh factor contains a high
47 abundance of n-alkanes and hopanes, and is identified to be vehicle exhaust (Pant and Harrison, 2013; Wang et al., 2017).
48 Coal combustion is identified by high loadings of Se, As and Pb (Chen et al., 2013; Wang et al., 2017), and the dust
49 factor is distinguished by crustal elements (ions) Ca, Si, and Ti. The cooking factor is distinguished by fatty acids (oleic
50 acid, palmitic acid and stearic acid) (Li et al., 2020). The fire working factor is identified by high loadings of flammable
51 metals such as Mg, Cu and Ba, etc.

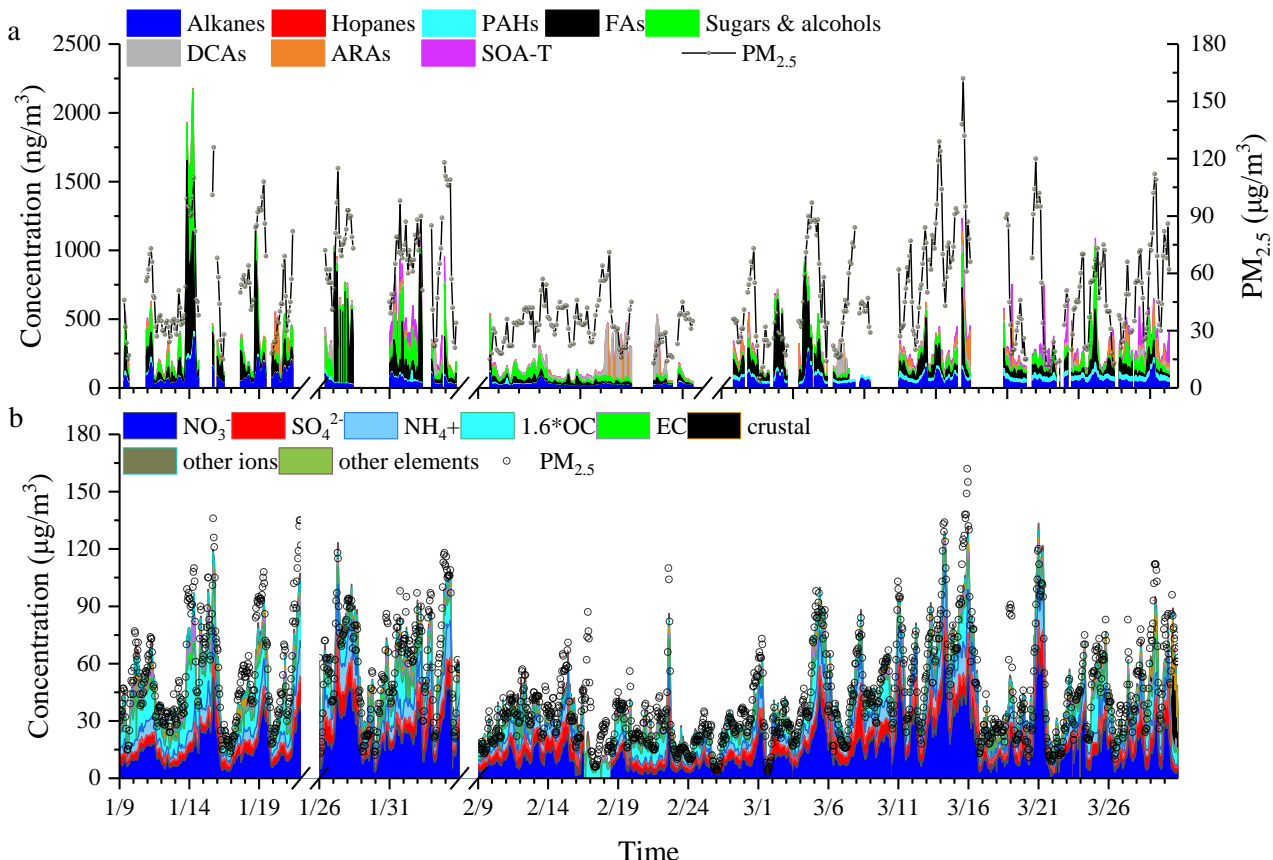
52

53

54

55 **Figure S1. Time series of PM_{2.5} and its components and organic molecular tracers.**

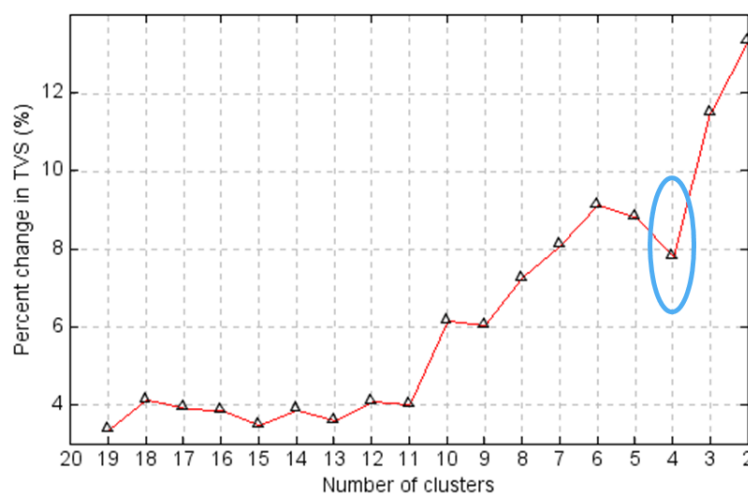
56 PAHs, polycyclic aromatic hydrocarbons; DCAs, dicarboxylic acids; FAs, fatty acids; ARAs, aromatic acids; SOA-T, secondary
 57 organic aerosol tracers; crustal=2.20×[Al]+2.49×[Si]+1.63×[Ca]+2.42×[Fe]+1.94×[Ti] ([Huang et al., 2014](#)).



58

59 **Figure S2. The variation of the total spatial variance.**

60 We choose the most appropriate clustering case based on the change in total spatial variance (TSV). The point raised
 61 down by TSV were selected as the optimal number of clusters, and the optimal solution of four clusters was finally
 62 extracted in this study ([He et al., 2020](#)).

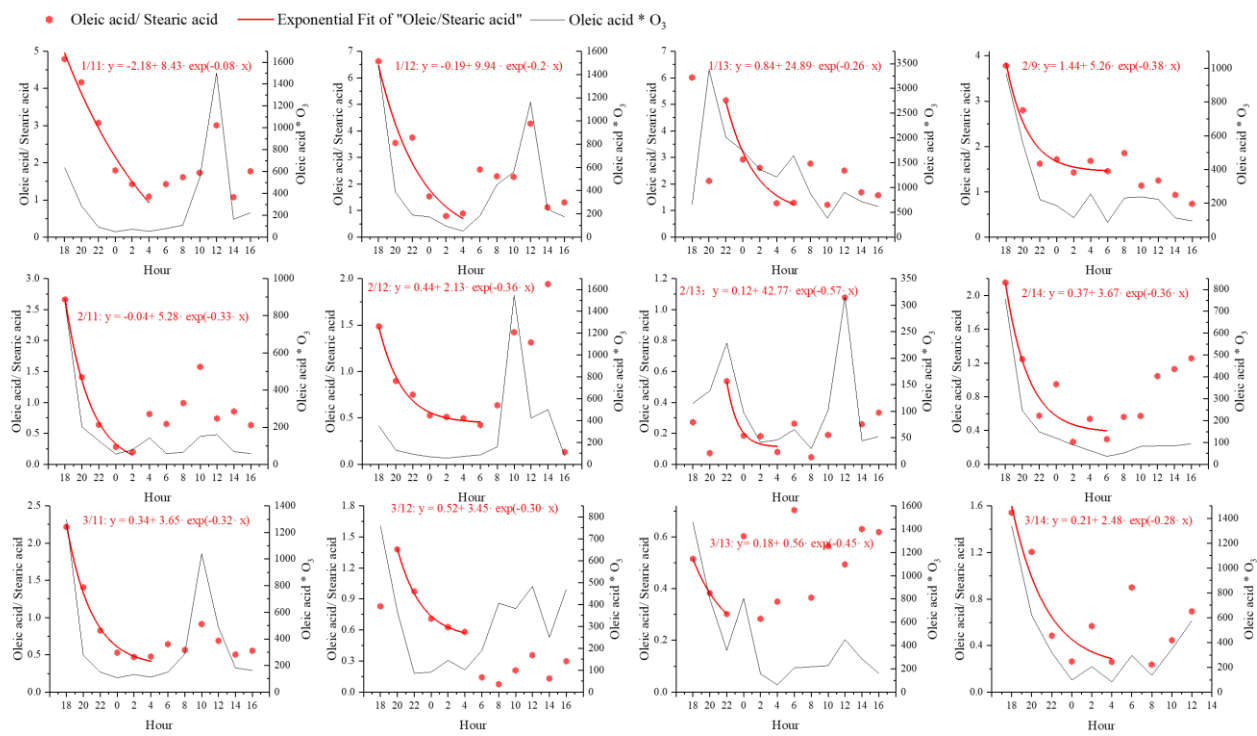
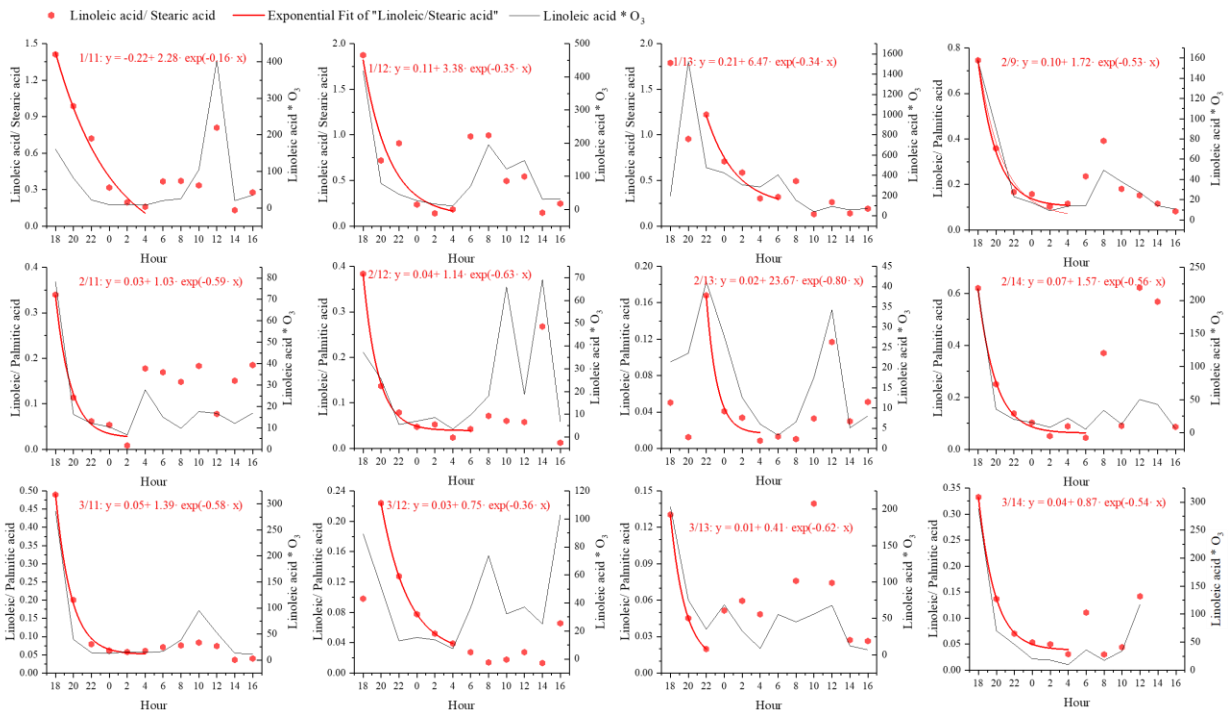


63

64

65

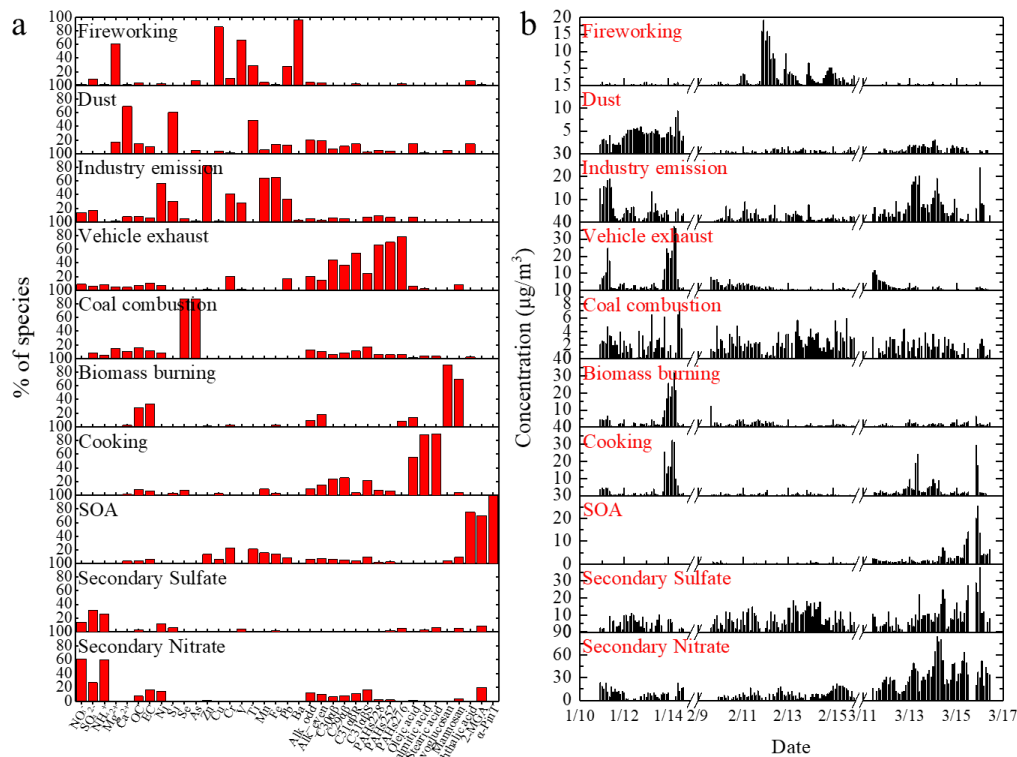
66

Figure S3. Day-to-day fitting of oleic acid normalized by palmitic acid.**Figure S4. Day-to-day fitting of linoleic acid normalized by palmitic acid.**

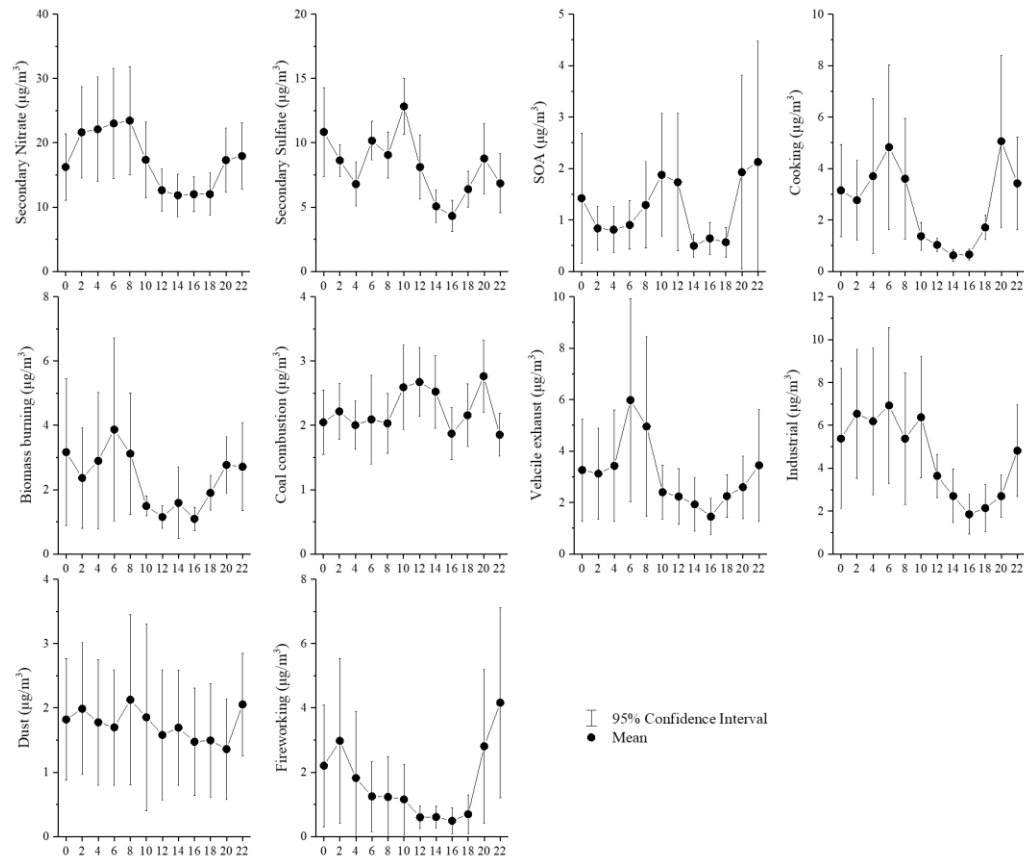
75

Figure S5. Individual source profiles of the 10 factors resolved in the PMF (a) and time series of individual factor contributions

76

(b).

77

Figure S6. Diurnal variation in individual source factors resolved by PMF.

79

Table S1. Contribution of TFAs to total OC (ng/μg) from different sources.

Sources	Min	Max	Avg	Std	References
Biomass Burning	6.6	25.8	14.5	5.8	(Hays et al., 2002; Schauer et al., 2001; Zhang et al., 2007)
Coal Combustion	3.9	29.9	11.6	9.9	(Zhang et al., 2008)
Vehicle Exhaust	0.32	6.2	2.6	2.1	(Cai et al., 2017)
Cooking	27.7	82.2	55.9	21.4	(Pei et al., 2016; Zhao et al., 2015; Zhao et al., 2007)

Table S2. PM_{2.5} and its components included in the PMF analysis (O₃ and NO₂ are not in PMF input).

naming	grouping	unit	concentration
Alk_odd	<i>n</i> -C ₂₅ , <i>n</i> -C ₂₇ , <i>n</i> -C ₂₉ , <i>n</i> -C ₃₁ and <i>n</i> -C ₃₃	ng/m ³	14.58
Alk_even	<i>n</i> -C ₂₄ , <i>n</i> -C ₂₆ , <i>n</i> -C ₂₈ , <i>n</i> -C ₃₀ and <i>n</i> -C ₃₂	ng/m ³	18.19
C30αβ	17α(H)21β(H)-hopane	ng/m ³	0.27
C29αβ	17α(H)21β(H)-30-norhopane	ng/m ³	0.20
C31αβR	17α(H)21β(H)-(22 <i>R</i>)-homohopane	ng/m ³	0.10
C31αβS	17α(H)21β(H)-(22 <i>S</i>)-homohopane	ng/m ³	0.23
PAHs228	Benzo[a]anthracene, Chrysene	ng/m ³	0.93
PAHs252	Benzo[b+k]fluoranthene, Benzo[a]pyrene	ng/m ³	1.32
PAHs276	Benzo[g,h,i]perylene, Indeno[1,2,3-cd]pyrene	ng/m ³	1.97
Oleic acid	Oleic acid	ng/m ³	32.15
Palmitic acid	Palmitic acid	ng/m ³	38.77
Stearic acid	Stearic acid	ng/m ³	26.51
Levoglucosan	Levoglucosan	ng/m ³	63.03
Mannosan	Mannosan	ng/m ³	3.82
Phthalic acid	Phthalic acid	ng/m ³	14.72
2-MGA	2-Methylglyceric acid	ng/m ³	2.06
α-PinT	3-Hydroxyglutaric acid, Pinic acid, Cis-pinonic acid	ng/m ³	10.26
NO ₃ ⁻		μg/m ³	17.28
SO ₄ ²⁻		μg/m ³	7.53
NH ₄ ⁺		μg/m ³	7.41
Other ions	Mg ²⁺ , Ca ²⁺	μg/m ³	0.52
OC		μg/m ³	6.73
EC		μg/m ³	2.20
Crustal elements	Si, Ti, Fe	μg/m ³	0.48
Other elements	Ni, Se, As, Zn, Cu, Cr, V, Mn, Pb, Ba	μg/m ³	1.34
PM _{2.5}		μg/m ³	50.07
O ₃		μg/m ³	51.53
NO ₂		μg/m ³	42.85

86

Table S3. Summary of error estimation diagnostics from BS, DISP and BS-DISP for PMF.

BS Mapping (R≥0.6)	Secondar y Nitrate	Secondar y Sulfate	SOA	Cooking	Biomass burning	Coal combusti on	Vehicle exhaust	Industry emission	Dust	Firework ing	Unmapp ed
SN	84	0	0	0	0	0	6	4	5	0	1
SS	0	83	0	0	0	7	0	6	0	0	4
SOA	0	0	98	1	0	0	0	0	0	0	1
Cooking	0	0	0	100	0	0	0	0	0	0	0
BB	0	0	0	0	99	0	0	1	0	0	0
CC	0	0	0	0	0	92	0	4	0	0	4
VE	0	0	0	0	0	0	96	2	0	0	2
In	0	0	0	0	0	0	0	100	0	0	0
Dust	0	0	0	0	0	0	0	0	100	0	0
Fire	0	0	0	0	0	0	0	0	0	100	0
DISP Diagnostics	Error Code: 0				Largest Decrease in Q: 0 (0%)						
Factor Swaps	dQ ^{max} =4	0	0	0	0	0	0	0	0	0	
	dQ ^{max} =8	0	0	0	0	0	0	0	0	0	
	dQ ^{max} =15	0	0	0	0	0	0	0	0	0	
	dQ ^{max} =25	0	0	0	0	0	0	0	0	0	
BS-DISP Diagnostics	# of runs accepted: 62 out of 101				Largest Decrease in Q: -20.938 (-0.43%)						
# of Decreases in Q: 8			# of Swaps in Best Fit: 21			# of Swaps in DISP: 10					
Factor Swaps	dQ ^{max} =0.5	5	8	9	26	15	1	11	8	12	7
	dQ ^{max} =1	5	8	9	26	15	1	12	8	13	7
	dQ ^{max} =2	7	8	10	28	15	1	13	8	17	8
	dQ ^{max} =4	7	10	13	32	16	2	14	9	21	11

87

88

89

90

91 **References**

- 92 Cai, T. Q., Zhang, Y., Fang, D. Q., Shang, J., Zhang, Y. X., and Zhang, Y. H.: Chinese vehicle emissions
93 characteristic testing with small sample size: Results and comparison, *Atmos Pollut Res*, 8(1), 154-163,
94 doi:10.1016/j.apr.2016.08.007, 2017.
- 95 Chen, J., Liu, G. J., Kang, Y., Wu, B., Sun, R. Y., Zhou, C. C., and Wu, D.: Atmospheric emissions of F, As, Se, Hg,
96 and Sb from coal-fired power and heat generation in China, *Chemosphere*, 90(6), 1925-1932,
97 doi:10.1016/j.chemosphere.2012.10.032, 2013.
- 98 Feng, J. L., Li, M., Zhang, P., Gong, S. Y., Zhong, M. A., Wu, M. H., Zheng, M., Chen, C. H., Wang, H. L., and Lou,
99 S. R.: Investigation of the sources and seasonal variations of secondary organic aerosols in PM2.5 in Shanghai with
100 organic tracers, *Atmos. Environ.*, 79, 614-622, doi:10.1016/j.atmosenv.2013.07.022, 2013.
- 101 Hays, M. D., Geron, C. D., Linna, K. J., Smith, N. D., and Schauer, J. J.: Speciation of gas-phase and fine particle
102 emissions from burning of foliar fuels, *Environmental Science & Technology*, 36(11), 2281-2295, doi:10.1021/es0111683,
103 2002.
- 104 He, X., Wang, Q. Q., Huang, X. H. H., Huang, D. D., Zhou, M., Qiao, L. P., Zhu, S. H., Ma, Y. G., Wang, H. L., Li,
105 L., Huang, C., Xu, W., Worsnop, D. R., Goldstein, A. H., and Yu, J. Z.: Hourly measurements of organic molecular
106 markers in urban Shanghai, China: Observation of enhanced formation of secondary organic aerosol during particulate
107 matter episodic periods, *Atmos. Environ.*, 240, doi:10.1016/j.atmosenv.2020.117807, 2020.
- 108 Huang, X. H. H., Bian, Q. J., Ng, W. M., Louie, P. K. K., and Yu, J. Z.: Characterization of PM2.5 Major
109 Components and Source Investigation in Suburban Hong Kong: A One Year Monitoring Study, *Aerosol Air Qual Res*,
110 14(1), 237-250, doi:10.4209/aaqr.2013.01.0020, 2014.
- 111 Li, R., Wang, Q. Q., He, X., Zhu, S. H., Zhang, K., Duan, Y. S., Fu, Q. Y., Qiao, L. P., Wang, Y. J., Huang, L., Li, L.,
112 and Yu, J. Z.: Source apportionment of PM2.5 in Shanghai based on hourly organic molecular markers and other source
113 tracers, *Atmos Chem Phys*, 20(20), 12047-12061, doi:10.5194/acp-20-12047-2020, 2020.
- 114 Men, C., Liu, R. M., Wang, Q. R., Guo, L. J., Miao, Y. X., and Shen, Z. Y.: Uncertainty analysis in source
115 apportionment of heavy metals in road dust based on positive matrix factorization model and geographic information
116 system, *Sci. Total Environ.*, 652, 27-39, doi:10.1016/j.scitotenv.2018.10.212, 2019.
- 117 Norris, G., Duvall, R., Brown, S., and Bai, S.: EPA Positive Matrix Factorization (PMF) 5.0 Fundamentals and User
118 Guide, 2014.
- 119 Pant, P., and Harrison, R. M.: Estimation of the contribution of road traffic emissions to particulate matter
120 concentrations from field measurements: A review, *Atmos. Environ.*, 77, 78-97, doi:10.1016/j.atmosenv.2013.04.028,
121 2013.
- 122 Pei, B., Cui, H. Y., Liu, H., and Yan, N. Q.: Chemical characteristics of fine particulate matter emitted from
123 commercial cooking, *Front Env Sci Eng*, 10(3), 559-568, doi:10.1007/s11783-016-0829-y, 2016.
- 124 Schauer, J. J., Kleeman, M. J., Cass, G. R., and Simoneit, B. R. T.: Measurement of emissions from air pollution
125 sources. 3. C-1-C-29 organic compounds from fireplace combustion of wood, *Environmental Science & Technology*,
126 35(9), 1716-1728, doi:10.1021/es001331e, 2001.
- 127 Wang, Q. Q., He, X., Huang, X. H. H., Griffith, S. M., Feng, Y. M., Zhang, T., Zhang, Q. Y., Wu, D., and Yu, J. Z.:
128 Impact of Secondary Organic Aerosol Tracers on Tracer-Based Source Apportionment of Organic Carbon and PM2.5: A
129 Case Study in the Pearl River Delta, China, *Acs Earth Space Chem*, 1(9), 562-571,
130 doi:10.1021/acsearthspacechem.7b00088, 2017.
- 131 Wang, Q. Q., Huang, X. H. H., Tam, F. C. V., Zhang, X. X., Liu, K. M., Yeung, C., Feng, Y. M., Cheng, Y. Y., Wong,
132 Y. K., Ng, W. M., Wu, C., Zhang, Q. Y., Zhang, T., Lau, N. T., Yuan, Z. B., Lau, A. K. H., and Yu, J. Z.: Source

133 apportionment of fine particulate matter in Macao, China with and without organic tracers: A comparative study using
134 positive matrix factorization, *Atmos. Environ.*, 198, 183-193, doi:10.1016/j.atmosenv.2018.10.057, 2019.

135 Zhang, Q., Ning, Z., Shen, Z. X., Li, G. L., Zhang, J. K., Lei, Y. L., Xu, H. M., Sun, J., Zhang, L. M., Westerdahl, D.,
136 Gali, N. K., and Gong, X. S.: Variations of aerosol size distribution, chemical composition and optical properties from
137 roadside to ambient environment: A case study in Hong Kong, China, *Atmos. Environ.*, 166, 234-243,
138 doi:10.1016/j.atmosenv.2017.07.030, 2017.

139 Zhang, Y. X., Schauer, J. J., Zhang, Y. H., Zeng, L. M., Wei, Y. J., Liu, Y., and Shao, M.: Characteristics of
140 particulate carbon emissions from real-world Chinese coal combustion, *Environmental Science & Technology*, 42(14),
141 5068-5073, doi:10.1021/es7022576, 2008.

142 Zhang, Y. X., Shao, M., Zhang, Y. H., Zeng, L. M., He, L. Y., Zhu, B., Wei, Y. J., and Zhu, X. L.: Source profiles of
143 particulate organic matters emitted from cereal straw burnings, *J Environ Sci*, 19(2), 167-175, doi:10.1016/S1001-
144 0742(07)60027-8, 2007.

145 Zhao, X. Y., Hu, Q. H., Wang, X. M., Ding, X., He, Q. F., Zhang, Z., Shen, R. Q., Lu, S. J., Liu, T. Y., Fu, X. X., and
146 Chen, L. G.: Composition profiles of organic aerosols from Chinese residential cooking: case study in urban Guangzhou,
147 south China, *J Atmos Chem*, 72(1), 1-18, doi:10.1007/s10874-015-9298-0, 2015.

148 Zhao, Y. L., Hu, M., Slanina, S., and Zhang, Y. H.: Chemical compositions of fine particulate organic matter emitted
149 from Chinese cooking, *Environmental Science & Technology*, 41(1), 99-105, doi:10.1021/es0614518, 2007.

150